

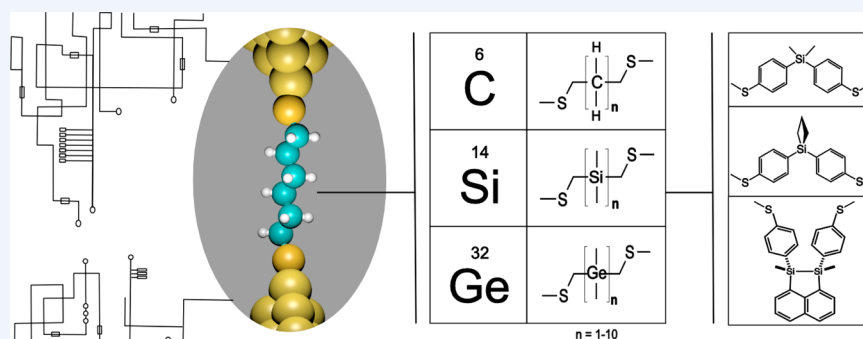
## Silane and Germane Molecular Electronics

Timothy A. Su,<sup>†</sup> Haixing Li,<sup>‡</sup> Rebekka S. Klausen,<sup>§</sup> Nathaniel T. Kim,<sup>†</sup> Madhav Neupane,<sup>†</sup> James L. Leighton,<sup>\*,†</sup> Michael L. Steigerwald,<sup>\*,†</sup> Latha Venkataraman,<sup>\*,†,‡</sup> and Colin Nuckolls<sup>\*,†</sup>

<sup>†</sup>Columbia University, Department of Chemistry, New York, New York 10027, United States

<sup>‡</sup>Columbia University, Department of Applied Physics and Applied Math, New York, New York 10027, United States

<sup>§</sup>Johns Hopkins University, Department of Chemistry, Baltimore, Maryland 21228, United States



**CONSPECTUS:** This Account provides an overview of our recent efforts to uncover the fundamental charge transport properties of Si–Si and Ge–Ge single bonds and introduce useful functions into group 14 molecular wires. We utilize the tools of chemical synthesis and a scanning tunneling microscopy-based break-junction technique to study the mechanism of charge transport in these molecular systems. We evaluated the fundamental ability of silicon, germanium, and carbon molecular wires to transport charge by comparing conductances within families of well-defined structures, the members of which differ only in the number of Si (or Ge or C) atoms in the wire. For each family, this procedure yielded a length-dependent conductance decay parameter,  $\beta$ . Comparison of the different  $\beta$  values demonstrates that Si–Si and Ge–Ge  $\sigma$  bonds are more conductive than the analogous C–C  $\sigma$  bonds. These molecular trends mirror what is seen in the bulk.

The conductance decay of Si and Ge-based wires is similar in magnitude to those from  $\pi$ -based molecular wires such as para-phenylenes. However, the chemistry of the linkers that attach the molecular wires to the electrodes has a large influence on the resulting  $\beta$  value. For example, Si- and Ge-based wires of many different lengths connected with a methyl–thiomethyl linker give  $\beta$  values of  $0.36\text{--}0.39\text{ \AA}^{-1}$ , whereas Si- and Ge-based wires connected with aryl–thiomethyl groups give drastically different  $\beta$  values for short and long wires. This observation inspired us to study molecular wires that are composed of both  $\pi$ - and  $\sigma$ -orbitals. The sequence and composition of group 14 atoms in the  $\sigma$  chain modulates the electronic coupling between the  $\pi$  end-groups and dictates the molecular conductance. The conductance behavior originates from the coupling between the subunits, which can be understood by considering periodic trends such as bond length, polarizability, and bond polarity.

We found that the same periodic trends determine the electric field-induced breakdown properties of individual Si–Si, Ge–Ge, Si–O, Si–C, and C–C bonds. Building from these studies, we have prepared a system that has two different, alternative conductance pathways. In this wire, we can intentionally break a labile, strained silicon–silicon bond and thereby shunt the current through the secondary conduction pathway. This type of *in situ* bond-rupture provides a new tool to study single molecule reactions that are induced by electric fields. Moreover, these studies provide guidance for designing dielectric materials as well as molecular devices that require stability under high voltage bias.

The fundamental studies on the structure/function relationships of the molecular wires have guided the design of new functional systems based on the Si- and Ge-based wires. For example, we exploited the principle of strain-induced Lewis acidity from reaction chemistry to design a single molecule switch that can be controllably switched between two conductive states by varying the distance between the tip and substrate electrodes. We found that the strain intrinsic to the disilaacenaphthene scaffold also creates two state conductance switching. Finally, we demonstrate the first example of a stereoelectronic conductance switch, and we demonstrate that the switching relies crucially on the electronic delocalization in Si–Si and Ge–Ge wire backbones. These studies illustrate the untapped potential in using Si- and Ge-based wires to design and control charge transport at the nanoscale and to allow quantum mechanics to be used as a tool to design ultraminiaturized switches.

Received: January 29, 2017

Published: March 27, 2017

## 1. INTRODUCTION

This Account describes a program we initiated several years ago to investigate molecular wires based on silanes and germanes using a scanning tunneling microscopy-based break-junction (STM-BJ) technique to measure conductance.<sup>1</sup> These studies were born from our interest in building an essential bridge between two distinct worlds: (1) the established semiconductor industry that transforms bulk silicon and germanium into nanoscale devices and (2) the emerging field of single-molecule electronics that aims to use individual molecules as the active elements in electrical circuitry (Figure 1). It is vital to link these

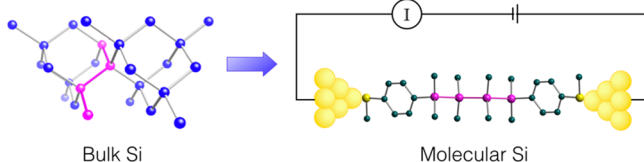


**Figure 1.** Studying molecular fragments of bulk silicon using the STM-BJ technique.

worlds because of the continued ultraminiaturization of silicon-based components and the issues and opportunities that arise from this device scaling. For example, how will the charge transport properties of the material change as the active regions transition from the nanoscale to the molecular scale? If we are to make these components from the bottom up, can we leverage our understanding of molecular chemistry to synthetically engineer function into the devices? Our hope is that the principal findings detailed in this Account will serve as an intellectual touchstone to address these important issues.

Group 14 materials have long been known to possess interesting electronic characteristics in the bulk.<sup>2,3</sup> For example, while alkanes do not absorb light at wavelengths longer than 190 nm, it was observed many years ago that oligosilanes and oligogermanes display strong absorbance in the range of 200–300 nm.<sup>4</sup> In a trend similar to linearly  $\pi$ -based systems,<sup>5</sup> the position of maximum absorbance and absorption coefficient increase with the length of the Si or Ge chain.<sup>6,7</sup> It was also shown that cyclic silanes have delocalized electrons<sup>8</sup> and that oligosilanes form charge transfer complexes with electron acceptors.<sup>9</sup> Silanes have been investigated as hole-transporting layers,<sup>10–12</sup> as UV emitters in OLEDs,<sup>13–15</sup> and as materials in photovoltaic cells.<sup>16,17</sup>

Excellent reviews and articles have been published on  $\sigma$  conjugation in oligosilanes and germanes, which we will not thoroughly discuss here due to space constraints.<sup>2,18,19</sup> Silanes and germanes are electroactive because of the delocalization that occurs in Si–Si and Ge–Ge  $\sigma$ -bonds due to the increased size, energy, and diffuseness of their atomic orbitals relative to C.<sup>20</sup> Michl, Tamao, and others have developed an understanding of the electronic delocalization in oligo- and polysilanes.<sup>2,19,21–23</sup> One particularly interesting aspect of Si- and Ge-based wires is that the conductance should depend strongly on the dihedral conformations along the chain.<sup>24</sup> The strongest coupling between subunits occurs when the silanes or germanes are oriented in an *anti* (dihedral = 180°) configuration; the weakest occurs when these dihedral angles are oriented in a *cis* configuration (dihedral = 0°).<sup>18,25</sup>

While the molecular conductance properties of many types of organic wires have been well studied,<sup>26–28</sup> there had been no experimental study on the use of wires containing sp<sup>3</sup>-hybridized

components such as the silanes and germanes, this despite promising theoretical work by Ratner and co-workers.<sup>24,29</sup>

We thus saw a tremendous opportunity in this unexplored class of molecular wires, and we set out to utilize the properties of silanes and germanes to create new single-molecule devices. This would allow us to test how the bulk properties of silanes and germanes may correlate with single molecule properties. We saw the scanning tunneling microscopy-based break-junction (STM-BJ) technique<sup>30</sup> as an ideal platform for studying these materials because it provides an instructive glimpse into how current flows through systems that are connected through rotatable bonds.<sup>31</sup> The pioneering Si–Si and Ge–Ge bond-forming work of Kumada, Tamao, Marschner, and others provided us with a synthetic toolkit to explore a diverse array of silicon and germanium-based structures.<sup>32–34</sup>

We divide the discussion below into two sections: one on the fundamental charge transport properties of these new molecular wires and a second on functional switches made from them. By measuring the length dependent decay constants ( $\beta$ ), we establish that Si–Si and Ge–Ge bonds are more conductive than the analogous C–C bonds, mirroring what is seen in bulk solids. The  $\beta$  values for the Si- and Ge-based wires are similar in magnitude to those from  $\pi$ -orbital-based molecular wires. However, the chemistry of the linkers that attach the molecular wires to the electrodes has a large influence on the resulting  $\beta$ -value. For example, Si- and Ge-based wires of many different lengths connected with a methyl–thiomethyl linker give a  $\beta$  value of 0.36–0.39 Å<sup>-1</sup>, whereas Si- and Ge-based wires connected with aryl–thiomethyl groups give drastically different  $\beta$ -values depending on the length of the chain. The conductance originates from the coupling between the subunits, which can be understood by considering trends such as bond length, polarizability, and bond polarity. The very same trends determine the voltage-induced breakdown properties of individual Si–Si, Ge–Ge, Si–O, Si–C, and C–C bonds.

We have been able to use the tools of physical organic chemistry to realize new types of switches that can be understood and appreciated at the orbital level. We find that including along the conduction path a silicon atom whose bonding environment is strained gives a molecular device that shows switchable conductance. We exploit such strain in silacyclobutane- and disilaacenaphthene-based wires to design single molecule devices that can switch conductance between two conductive states by varying the distance between the tip and substrate electrodes. Finally, we demonstrate the first example of a stereoelectronic conductance switch that relies crucially on the electronic delocalization in Si–Si and Ge–Ge wire backbones.

## 2. FUNDAMENTALS OF SINGLE-MOLECULE CHARGE TRANSPORT IN SI- AND GE-BASED WIRES

### 2.1. $\beta$ -Values

The use of single molecules as active components in miniaturized electronic circuits requires a detailed understanding of the charge transport ability. One parameter that describes the efficacy of charge transport at the molecular scale is the  $\beta$ -value, which has units of inverse length.<sup>26,35</sup> The  $\beta$ -value and the length ( $L$ ) of a molecular wire conducting by a nonresonant tunneling mechanism are related exponentially ( $G \approx e^{-\beta L}$ , where  $G$  = conductance).<sup>28</sup> The decay constant depends on the coupling strength between the repeat units in any given material: molecular backbones that are strongly coupled and transport charge effectively give shallow conductance decay and lower  $\beta$  values.

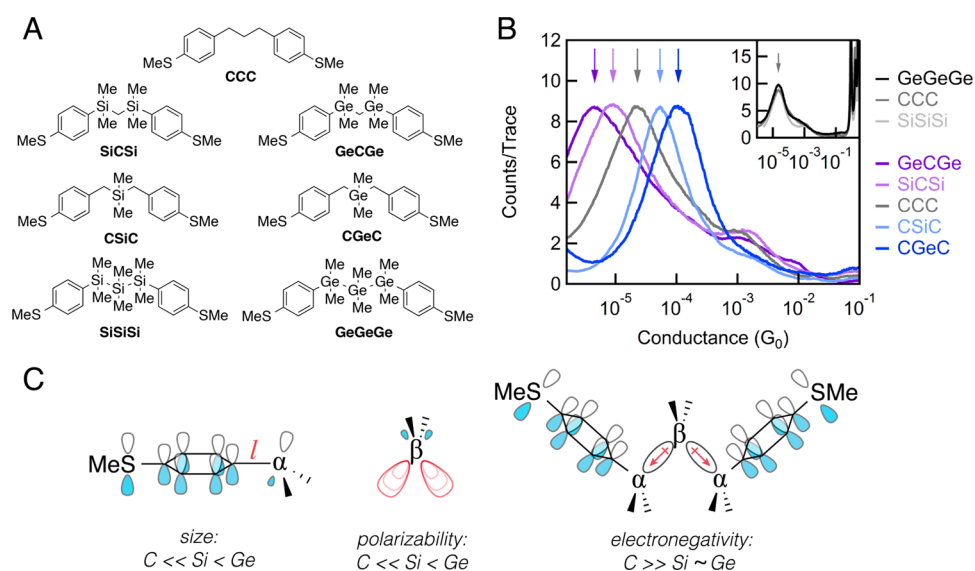


**Figure 2.** (A) Molecular structures with different  $\alpha$ - $\beta$ - $\alpha$  chains. (B) Conductance histograms for the  $\alpha$ - $\beta$ - $\alpha$  chains. (C) Periodic trends in the central  $\sigma$ -chain control the strength of coupling between the thioanisole rings.

Our initial objective was to explore whether permethylated oligosilanes, which have been shown to be electroactive in bulk,<sup>36,37</sup> would display molecular conductance similar to the  $\pi$ -conjugated carbon analogues such as paraphenylenes ( $\beta = 0.40 \text{ \AA}^{-1}$ )<sup>38</sup> and oligoenes ( $\beta = 0.22 \text{ \AA}^{-1}$ ).<sup>39,40</sup> We developed syntheses for long ( $>2 \text{ nm}$ ) molecular wires initially using thioanisole linkers paired with permethyloligosilane ( $-\text{[SiMe}_2\text{]}_n-$ ) backbones. However, this system gave different  $\beta$ -values for shorter ( $n = 1-4$ ;  $\beta = 0.27 \text{ \AA}^{-1}$ ) and longer ( $n = 4-6$ ,  $\beta = 0.46 \text{ \AA}^{-1}$ ) oligomers.<sup>37</sup> We observed similar inconsistencies in the  $\beta$ -values of short and long oligogermanes we had synthesized with thioanisole linkers. We reasoned that with thioanisole, linkers have a larger effect and a greater energetic mismatch with the shorter oligomers than the longer oligomers, where the central  $\sigma$ -orbitals play a larger role.

To help understand why the aromatic linkers at the ends of the silicon or germanium chain had such a big effect on the  $\beta$  values for the short silicon and germanium chains we prepared the series of test molecules shown in Figure 2.<sup>41</sup> Little was known regarding the transport and conductance properties of mixed  $\sigma$ - $\pi$  backbone wires. In these wires, the thioanisole rings connect the  $\sigma$ -moiety (a triatomic  $\alpha$ - $\beta$ - $\alpha$  chain composed of C, Si, or Ge atoms) to the electrodes. Figure 2B displays the conductance histograms for five different molecular wires. We found that the sequence and composition of group 14 atoms in the  $\alpha$ - $\beta$ - $\alpha$  chain dictated whether electronic communication between the aryl rings was enhanced or suppressed. Placing heavy atoms at the  $\alpha$ -position decreased conductance, whereas placing them at the  $\beta$ -position increased conductance: for example, the C-Ge-C sequence was found to be more than 20 times more conductive than the Ge-C-Ge sequence. There is a stronger interaction between the  $\pi$ -system and  $\sigma$ -chain for CGeC compared to GeCGe for three primary reasons, as shown in Figure 2c: (1) the Ar-C bond ( $1.5 \text{ \AA}$ ) is significantly shorter than the Ar-Ge bond ( $2.0 \text{ \AA}$ ), which brings the arene into closer interaction with the  $\sigma$ -chain for CGeC; (2) the Ge atom in the  $\beta$ -position is more polarizable, and (3) the stronger electronegativity of C relative to Ge polarizes the C-Ge bond density toward the aryl ring in CGeC but away the aryl ring in GeCGe. Interestingly, the periodic trends that control molecular conductance here are

the same ones that give rise to the  $\alpha$  and  $\beta$  silicon effects known to physical organic chemistry.<sup>42-44</sup> These findings provide a new molecular design concept for tuning conductance in single-molecule electrical devices<sup>45</sup> and demonstrate how principles of physical/mechanistic chemistry can be harnessed in designing molecules and tuning molecular conductance.

By replacing the phenylene spacer of the thioanisole linker with a methylene, we were able to access a more intrinsic, length-independent  $\beta$  value for the wires. Through single-molecule conductance measurements, we were able to establish that Si-Si and Ge-Ge bonds are more conducive to charge transport than the analogous C-C bonds ( $\beta_{\text{Ge}} = 0.36 \text{ \AA}^{-1}$ ,  $\beta_{\text{Si}} = 0.39 \text{ \AA}^{-1}$ ,  $\beta_{\text{C}} = 0.74 \text{ \AA}^{-1}$ , Figure 3).<sup>47</sup> These conductivity trends arise from the delocalization in the Si-Si and Ge-Ge  $\sigma$ -bonds—the very same delocalization that enables the widespread utility of bulk silicon and bulk germanium as semiconducting materials.

The periodic trends in molecular conductivity that we observed mirror group 14 conductivity trends in solid-state materials (Figure 3C); the bulk conductivities of silicon and germanium are the same order of magnitude, and both are much more conductive than diamond carbon.<sup>46</sup> These trends are not mirrored in stochastically grown Si and Ge nanowires where reported conductivities vary by many orders of magnitude due to a number of extrinsic factors.<sup>48-51</sup> The atomic precision in the molecular wires described here makes them reliable platforms for studying effects such as strain and doping in electronic materials, not only to probe the fundamental nature of these effects in bulk systems but also to inform the design of next-generation electronic materials.

## 2.2. Electrochemical Field Breakdown of Molecular Junctions

The implementation of low- $\kappa$  dielectric materials has been vital to increasing the density of semiconductor components on a chip. However, low- $\kappa$  dielectrics are more fragile than conventional dielectric materials. Many theoretical models have been developed to rationalize electric field breakdown in silicon-based networks of low- $\kappa$  materials, but an experimental study of voltage-induced breakdown at the single-bond level was lacking. Voltage-induced electric field breakdown experiments in single-molecule junctions can serve as a guide in designing low- $\kappa$



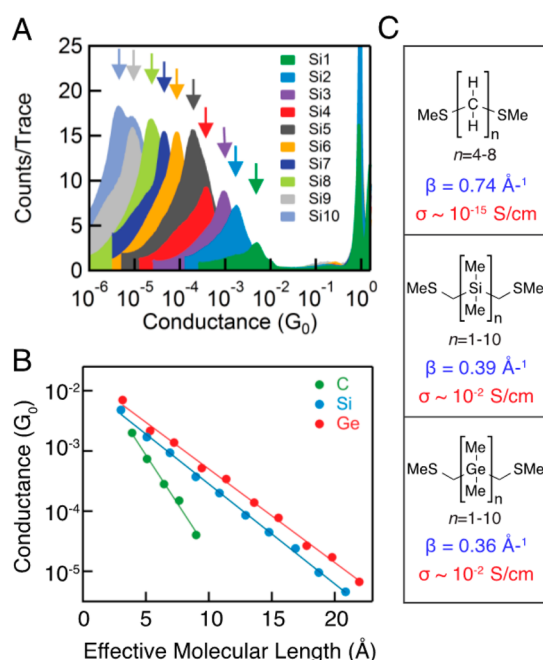


**Figure 3.** (A) Conductance histograms (Si1 to Si10) with methylthiomethyl linkers. (B) Conductance peak positions of the alkanes, oligosilanes, and oligogermanes plotted against  $L$  to give the  $\beta$ -value. (C) Trends in  $\beta$  value for the molecular materials mirror the conductivity trends observed for the bulk material. The  $\beta$  values of the alkane, silane, and germane oligomers are given in blue, and the conductivity values of the bulk materials<sup>46</sup> are given in red.

dielectric materials for electronic devices while developing a mechanistic understanding of a voltage-induced bond rupture process. To address this, we synthesized molecular analogs of low- $\kappa$  dielectric materials, now using thiol-based anchoring groups, since they form more robust Au–S covalent contacts than thioethers.<sup>52</sup> We used the junction rupture probability to assess the stability of Si–Si, Ge–Ge, C–C, Si–C, and Si–O bonds under high voltage bias and discovered that the probability of a bond to rupture can be related to its polarizability as well as its polarity (Figure 4).

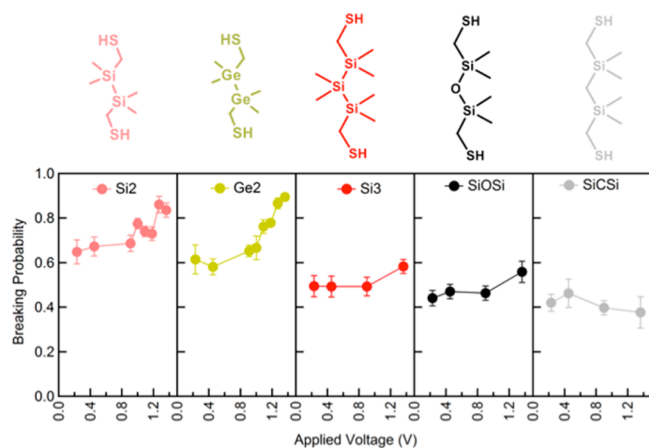


**Figure 4.** Molecular junction rupture probability plotted against the applied voltage for different backbones. The hold period for evaluating junction breakdown was 150 ms.

We considered molecular backbones that consist of Si–Si, Si–C, Si–O, and Ge–Ge bonds (Figure 4) and found that the

stability of bonds followed the trend C–C > Si–Si > Ge–Ge. This trend scales with characteristic bond strengths and polarizabilities of group 14 compounds. Furthermore, we found that molecular backbones with Si–C bonds have a lower breaking probability at a high voltage when compared with backbones with Si–O and Si–Si bonds. Indeed, Si–C and Si–O bonds are common in high performance dielectric materials; these studies suggest that such voltage-induced breakdown studies can provide a roadmap for designing low- $\kappa$  dielectric materials as well as molecular devices that require stability under high voltage bias.

We applied the same high-voltage experimental technique to a study of the impact of ring strain on bond-rupture probability, with an eye toward performing *in situ* chemistry within a single-molecule junction.<sup>53</sup> The prospect of forming a stable molecular junction and then inducing the making or breaking of chemical bonds through the application of external stimuli is exciting and holds the promise of new types functional components in single molecule circuits and the ability to study fundamental reactions on single molecules.

We chose to study the disilanaphthene system to probe Si–Si bond rupture because it contains two possible conductance pathways. Our hypothesis was that field-induced rupture of the strained, high-energy Si–Si bond should redirect the primary transport pathway through the alternate arene pathway (Figure 5A). In Figure 5B, we show that the Si–Si bond in disilaacenaphthene is ruptured under high bias, and this bond cleavage yields not a broken junction but rather a new conducting species whose likely post-rupture conductance pathway uses the 1,8-naphthadiyl subsystem. From calculations and simulations, we find that tunneling electrons excite molecular vibrational modes leading to homolytic Si–Si bond cleavage.

We are currently studying the homolytic Si–Si bond rupture event to understand the fate of the diradical that forms upon bond cleavage. The individual conductance traces (Figure 5B) reveal that the ruptured species persists even after the voltage is reduced, and the junction only breaks when the electrodes are pulled further apart. This raises an important question about why the Si–Si bond does not simply reform once the voltage is reduced. Our ongoing hypothesis is that the bond rupture is partly driven by strain relief and is accompanied by conformational relaxation that could preclude Si–Si bond reformation.

### 3. INCORPORATING FUNCTION INTO THE GROUP 14 MOLECULAR WIRES

Section 2 of this manuscript focused on the fundamental electronic properties of silanes and germanes and how these properties contribute to their mechanism of charge transport at the molecular scale. This section will focus on how those properties, in conjunction with our expertise in molecular design, have allowed us to create new types of conductance switches.

#### 3.1. Strain Induced Molecular Switching in Silacyclobutanes

State of the art technology in the semiconductor industry incorporates strain in the silicon crystal lattice to improve charge mobility and channel conductance.<sup>54</sup> To gain insight into the impact of strain at the molecular level, we set out to explore the impact of ring strain on the single molecule conductance properties of silanes. Ring strain in silacyclobutanes induces synthetically useful levels of reactivity in otherwise unreactive silanes.<sup>55–57</sup> We began by exploring the conductance properties of the bisthioanisole-equipped silacyclobutane (Figure 6).<sup>58</sup> With this strained silacycle, the molecular wire conducts not only from the terminal sulfur-to-sulfur, but also from sulfur-to-silacycle.

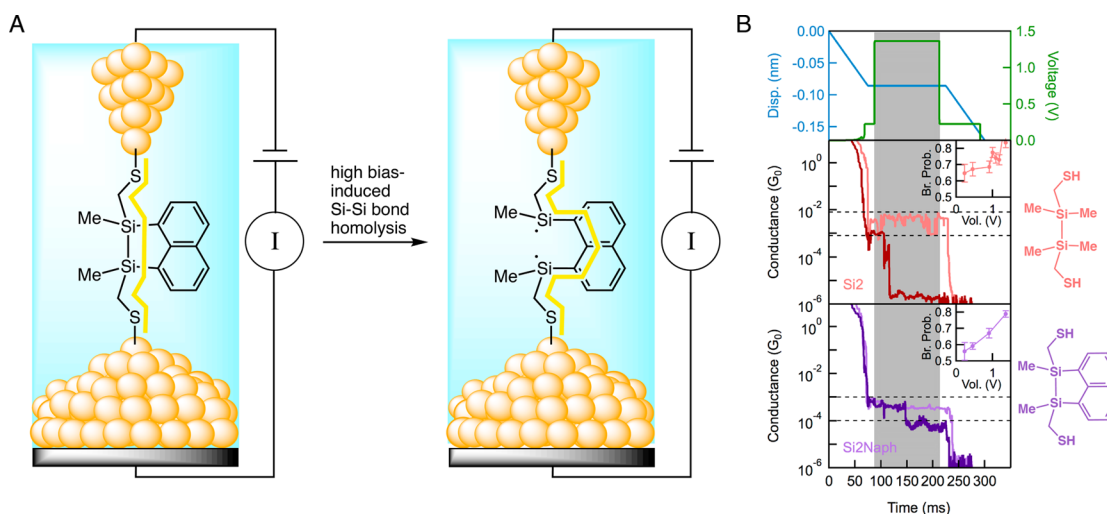


**Figure 5.** (A) Schematic of Si–Si bond rupture under applied voltage. The conductance occurs through an alternate pathway upon bond rupture. (B) Unlike the linear disilane (red), the cyclic disilane (purple) yields a new conductance plateau upon bond rupture.

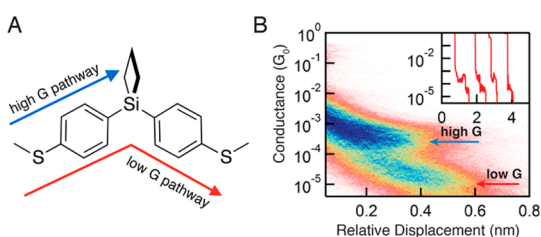


**Figure 6.** (A) Schematic of strained silane with both a high and a low conductance pathway. (B) 2D histogram with two distinct conductance states at specific tip–substrate electrode distances. Inset: individual traces demonstrating two-state conductance switching.

As indicated in the 2D histogram (Figure 6), we observe two different conductance states (high  $G$  and low  $G$ ) that differ at least by an order of magnitude. We can switch between pathways in a single junction by modulating the tip–substrate electrode distance.

We speculate that the contact for the high  $G$  pathway is a  $\sigma$ -complex formed between the strained, high-energy Si–C bond and the unsaturated gold electrode. The 0.4 nm elongation length obtained from the 2D histogram corresponds to the distance between the terminal sulfur and the carbon atom of the silacyclobutane moiety. Our studies uncovered the electronic effects of straining silicon at the molecular level and provide a foundation for the realization of strained silicon molecular components.

### 3.2. High Conductance Pathways in Ring-Strained Disilanes

Building from the demonstration that the ring strain in a silacyclobutane allowed a stable electrical contact to form, we have been exploring the impact of a different kind of ring strain on disilanes by synthesizing and characterizing disilaacenaphthenes equipped with thioanisole anchor groups.<sup>59</sup> We found that whereas the *trans* diastereomer (*trans*-Si2Naph) displays only the expected low  $G$  sulfur-to-sulfur pathway, the *cis* diastereomer (*cis*-Si2Naph) shows a prominent high  $G$  pathway as the primary conductance band along with a minor low  $G$ , sulfur-to-sulfur, peak (Figure 7). A novel bipodal binding mode wherein both thioanisole groups coordinate to the gold substrate would significantly reduce the entropic cost of establishing an otherwise too-weak-to-form electrical contact between the strained Si–Si bond and the gold electrode. Such a contact may be understood as a  $\sigma$ -complex and strongly suggests that we are observing a direct Si to Au contact in single molecule circuits, similar to what has been observed in Au-mediated organosilane reaction chemistry.<sup>60</sup>

### 3.3. Stereoelectronic Switching

Oligosilane and oligogermane with methylthiomethyl ( $\text{CH}_2\text{SMe}$ ) linkers (from section 2) display a unique mode of molecular switching when probed by an STM-BJ platform.<sup>47,61</sup> We term this phenomenon stereoelectronic switching because it originates from the stereoelectronic properties of the sulfur–methylene  $\sigma$ -bonds. The strongly coupled Si–Si and Ge–Ge  $\sigma$ -bonds enable

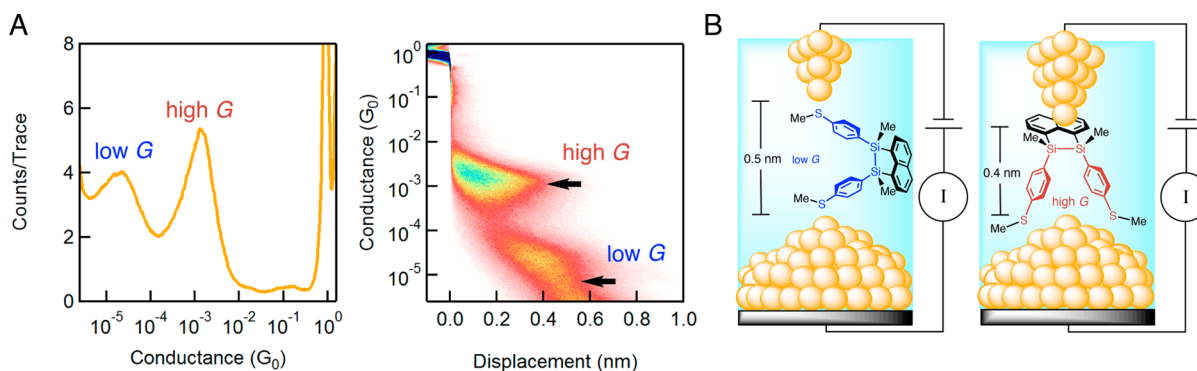


**Figure 7.** (A) 1D (left) and 2D histograms (right) that show distinct conductance states for *cis*-dithioanisole–disilaacenaphthene. (B) Schematic for two binding modes that give rise to the two low- and high-conductance states.

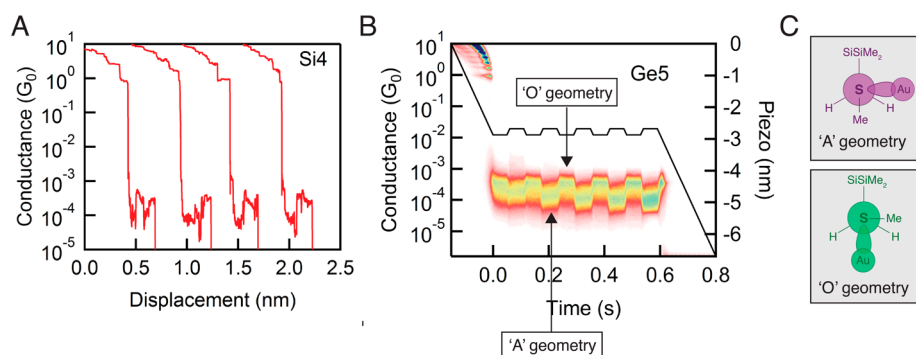


**Figure 8.** (A) Individual conductance traces for Si4 with methylthiomethyl linkers showing an increase in conductance with junction elongation. (B) 2D histogram of five compression/elongation cycles for the Au–Ge5–Au junction. A modified piezo ramp (black line) is applied to induce switching. (C) The orbitals on the linker sulfur of the linker provide a stereoelectronic effect to switch conductance. In the “O” geometry the p-orbital of the S atom is aligned with the silane chain, and when in the “A” geometry, conductance is turned off.

this mode of switching because they electronically couple the behavior of the linker groups at each end of the molecule. We will focus here on the oligosilane system, though these effects are even stronger in the oligogermanes, due to the stronger coupling in the Ge–Ge backbone.

Unlike most molecular junctions where conductance decreases as the molecular junction is elongated, the molecular systems Si1–Si10 show an abrupt jump from a lower to higher conductance upon elongation (Figure 8A). The molecular switching process we observe here is robust and reversible and can be exercised in real time (Figure 8B). We found that we could switch between a high *G* state and low *G* state by elongating or compressing the molecular junction by 2 Å. Furthermore, we found that our junctions behaved as better and better switches with each successive compression–elongation cycle, where the average conductance difference between the two states increases after each cycle. These cycles mechanically anneal the electrodes into an optimal structure for stereoelectronic switching and enable the junction to distinguish molecular conformations with more clarity.

The molecular switching in Si1–Si10 is caused by a stereoelectronic effect of the two terminal dihedral angles ( $\text{H}_3\text{C}-\text{S}-\text{CH}_2-\text{SiMe}_2$ ) that couple the molecule to the gold electrodes. These terminal dihedral angles should be particularly sensitive to changes in the molecular junction length because of the torque exerted on the molecule by the electrodes via the sulfur lone pair. There are two significant observations that support our argument. First, for all oligosilanes Si1–Si10, the conductance changes by a factor of 2 regardless of the oligosilane chain length. Second, the length of the conductance plateau corresponding the low conductance state increases from Si1 to Si10 (1 Å for Si1 to 10 Å for Si10) while that of the high *G* state stays relatively constant (1.5–2.0 Å). This consistency in the switching ratio and high *G* length across the entire oligosilane series suggests that the high *G* state arises from a molecular feature that is common to all oligomers like the stereoelectronic nature of the terminal dihedrals and not from the rotation of internal Si–Si–Si–Si dihedrals.

DFT-based analysis of a Au–Si4–Au model system reveals that there are two distinct Me–S–CH<sub>2</sub>–SiMe<sub>2</sub> dihedral geometries: an *anti* geometry where the Me group is antiperiplanar (Au atom is orthogonal) to the SiMe<sub>2</sub> group and an *ortho* geometry where the Me group is orthogonal (Au atom is antiperiplanar) to the SiMe<sub>2</sub> group. Each terminal Me–S–CH<sub>2</sub>–SiMe<sub>2</sub> dihedral angle that couples the electrode-linker orbital into the  $\sigma$  framework acts as a gate to control conductance.

At short interelectrode distances, steric strain predisposes the S–methyl bond in the *anti* geometry (Figure 8C) to minimize steric repulsion between the bulky S–methyl and the SiMe<sub>2</sub> groups. As the junction elongates, mechanical strain pulls the S–Au bond into the *ortho* geometry (Figure 8C) to adopt the longest possible molecular geometry—this geometry also maximizes conductance. The subangstrom level of control facilitated by the STM-BJ technique allowed us to manipulate these specific dihedrals in the molecular junction. As a result, the molecular conductance can be increased or decreased simply by elongating or compressing the molecular junction. These studies also reinforce how the principles of physical organic chemistry can be applied to create single molecule electronic devices.

#### 4. SUMMARY AND OUTLOOK

These studies detail a rich, new vein of research in the single molecule conductance of silicon- and germanium-based systems. The rotatable bonds in these systems allow access to low- and high-conductance through mechanically enforced quantum interference. One could imagine that the mechanically triggered conductance switches described here may serve as useful scaffolds for devices that essentially serve as molecular strain gauges that report on molecular scale force events. Holding the silanes in well-defined conformations in cages and cycles will provide interesting results that further expand the comparison between bulk silicon and single molecule devices by testing larger fragments. It is also clear that the contact between these wires and the electrodes is important. One area of exploration is how the more reactive stannanes, which are known to bond directly to gold electrodes in the STM-BJ, can be incorporated into these molecular systems.<sup>62</sup> We are also exploring how we can effectively “dope” our wires with appropriate substituents pendant to the silicon or germanium chains. Finally, we envision that many more conformational switches will be developed for these systems that share the same tetrahedral bonding geometry as alkanes. We imagine that the numerous stereoelectronic models proposed for understanding the reaction chemistry of alkanes can be similarly applied to silanes to create new types of conductance switches.

#### ■ AUTHOR INFORMATION

##### Corresponding Authors

\*E-mail: jll43@columbia.edu.

\*E-mail: mls2064@columbia.edu.

\*E-mail: lv2117@columbia.edu.



\*E-mail: [cn37@columbia.edu](mailto:cn37@columbia.edu).

ORCID 

Haixing Li: 0000-0002-1383-4907

James L. Leighton: 0000-0002-9061-8327

Latha Venkataraman: 0000-0002-6957-6089

Colin Nuckolls: 0000-0002-0384-5493

## Notes

The authors declare no competing financial interest.

## Biographies

**Timothy Su** was born in Dhahran, Saudi Arabia, in 1989. He completed his undergraduate studies with Jean Fréchet at UC Berkeley, then received his Ph. D. in 2016 with Colin Nuckolls at Columbia University as an NSF Graduate Fellow. He is currently an NIH postdoctoral fellow with Chris Chang at UC Berkeley.

**Haixing Li** was born in China in 1990. She completed her undergraduate studies at University of Science and Technology of China with Xianhui Chen and now is a Ph.D. candidate working with Latha Venkataraman at Columbia University.

**Rebekka Klausen** was born in Brooklyn, New York, in 1983. She earned her B.S. at Boston College in 2005 working with Steven Bruner. After completing graduate training with Eric N. Jacobsen at Harvard University (2005–2011), she was a postdoctoral scholar with Colin Nuckolls at Columbia University (2011–2013). She is currently an assistant professor at Johns Hopkins University in Baltimore, MD.

**Nathaniel Kim** was born in Seoul, South Korea, in 1989. He completed his undergraduate studies at the University of Maryland, Baltimore County, with Katherine Seley-Radtke, and then received his Ph. D. in 2016 from Columbia University with James Leighton. He is currently a lecturer in discipline at Columbia University.

**Madhav Neupane** was born in western Nepal in 1987. He completed his undergraduate studies from Texas A&M University in 2013 working under John A. Gladysz. He is currently a fourth year graduate student working with Colin Nuckolls at Columbia University.

**James Leighton** was born in Connecticut in 1964. He did his undergraduate studies at Yale University with Samuel Danishefsky and received his Ph.D. from Harvard University in 1994 with David Evans. Following an NSF postdoctoral fellowship with Eric Jacobsen, he joined the faculty at Columbia University in 1996. He was promoted to the rank of Professor in 2004 and is currently serving as Department Chair.

**Michael Steigerwald** was born in Michigan in 1956. He did both his undergraduate and graduate training at Caltech, working with David Evans, Bill Goddard, and Bob Grubbs. After a postdoctoral stay with Marty Semmelhack at Princeton, he joined Bell Laboratories where he worked in solid-state chemistry. He has been at Columbia since 2002 as a research scientist.

**Latha Venkataraman** earned her Ph.D. with Charles Lieber at Harvard University in 1999. She joined Columbia University as a research scientist in 2003 and started as an assistant professor in 2007. She is currently Professor of Applied Physics and Chemistry.

**Colin Nuckolls** was born in Great Britain in 1970. He completed his undergraduate studies at UT Austin with Marye Anne Fox, and then received his Ph.D. in 1998 from Columbia University with Thomas Katz. He was an NIH postdoctoral fellow with Julius Rebek, Jr., at the Scripps Research Institute. He joined the faculty at Columbia University in 2000, and in 2006, he was promoted to the rank of Professor. He is currently the Sheldon and Dorothea Buckler Professor of Materials Science.

## ACKNOWLEDGMENTS

We thank the National Science Foundation for the support of this work under Grant CHE-1404922. T.A.S. was supported by the NSF Graduate Research Fellowship under Grant No. 11-44155. H.L. is supported in part by the Semiconductor Research Corporation and New York Center for Advanced Interconnect Science and Technology Program. C.N. thanks Sheldon and Dorothea Buckler for their generous support. The Columbia University Shared Materials Characterization Laboratory (SMCL) was used extensively for this research. We are grateful to Columbia University for support of this facility.

## REFERENCES

- (1) Klausen, R. S.; Widawsky, J. R.; Steigerwald, M. L.; Venkataraman, L.; Nuckolls, C. Conductive Molecular Silicon. *J. Am. Chem. Soc.* **2012**, *134*, 4541–4544.
- (2) Miller, R. D.; Michl, J. Polysilane High Polymers. *Chem. Rev.* **1989**, *89*, 1359–1410.
- (3) Jones, R. G.; Ando, W.; Chojnowski, J. *Silicon-Containing Polymers: The Science and Technology of Their Synthesis and Applications*; Springer Science & Business Media, 2013.
- (4) Gilman, H.; Atwell, W. H.; Schwebke, G. L. Ultraviolet Properties of Compounds Containing the Silicon-Silicon Bond. *J. Organomet. Chem.* **1964**, *2*, 369–371.
- (5) Hausser, R. W.; Kuhn, R.; Smakula, A. Photoabsorption and Double Bonding in Diphenyl-Polyene. *Z. Phys. Chem.* **1935**, *29B*, 384–389.
- (6) West, R.; Carberry, E. Permethylpolysilanes - Silicon Analogs of Hydrocarbons. *Science* **1975**, *189*, 179–186.
- (7) Gilman, H.; Morris, P. J. Ultraviolet Spectra of Some Pentahalophenyl-Substituted Silanes. *J. Organomet. Chem.* **1966**, *6*, 102–104.
- (8) Carberry, E.; West, R.; Glass, G. E. Cyclic Polysilanes. IV. Anion Radicals and Spectroscopic Properties of Permethylcyclopolysilanes. *J. Am. Chem. Soc.* **1969**, *91*, 5446–5451.
- (9) Traven, V. F.; West, R. Charge-Transfer Complexing between Permethylpolysilanes and Tetraethylene. *J. Am. Chem. Soc.* **1973**, *95*, 6824–6826.
- (10) Kido, J.; Nagai, K.; Okamoto, Y.; Skotheim, T. Poly-(Methylphenylsilane) Film as a Hole Transport Layer in Electroluminescent Devices. *Appl. Phys. Lett.* **1991**, *59*, 2760–2762.
- (11) Suzuki, H.; Meyer, H.; Simmerer, J.; Yang, J.; Haarer, D. Electroluminescent Devices Based on Poly(Methylphenylsilane). *Adv. Mater.* **1993**, *5*, 743–746.
- (12) Kitao, T.; Bracco, S.; Comotti, A.; Sozzani, P.; Naito, M.; Seki, S.; Uemura, T.; Kitagawa, S. Confinement of Single Polysilane Chains in Coordination Nanospaces. *J. Am. Chem. Soc.* **2015**, *137*, 5231–5238.
- (13) Fujii, A.; Yoshimoto, K.; Yoshida, M.; Ohmori, Y.; Yoshino, K. Ultraviolet Electroluminescent Diode Utilizing Poly-(Methylphenylsilane). *Jpn. J. Appl. Phys.* **2 1995**, *34*, L1365–L1367.
- (14) Xu, Y. H.; Fujino, T.; Naito, H.; Oka, K.; Dohmaru, T. Room Temperature Ultraviolet Electroluminescence from Poly-(Methylphenylsilane). *Chem. Lett.* **1998**, *27*, 299–300.
- (15) Yuan, C. H.; Hoshino, S.; Toyoda, S.; Suzuki, H.; Fujiki, M.; Matsumoto, N. Room-Temperature near-Ultraviolet Electroluminescence from a Linear Silicon Chain. *Appl. Phys. Lett.* **1997**, *71*, 3326–3328.
- (16) Okumoto, H.; Yatabe, T.; Richter, A.; Peng, J. B.; Shimomura, M.; Kaito, A.; Minami, N. A Strong Correlation between the Hole Mobility and Silicon Chain Length in Oligosilane Self-Organized Thin Films. *Adv. Mater.* **2003**, *15*, 716–720.
- (17) Lee, J. H.; Seoul, C.; Park, J. K.; Youk, J. H. Fullerene/Poly(Methylphenylsilane) (Pmps) Organic Photovoltaic Cells. *Synth. Met.* **2004**, *145*, 11–14.
- (18) Tsuji, H.; Michl, J.; Tamao, K. Recent Experimental and Theoretical Aspects of the Conformational Dependence of UV Absorption of Short Chain Peralkylated Oligosilanes. *J. Organomet. Chem.* **2003**, *685*, 9–14.

- (19) Schepers, T.; Michl, J. Optimized Ladder C and Ladder H Models for Sigma Conjugation: Chain Segmentation in Polysilanes. *J. Phys. Org. Chem.* **2002**, *15*, 490–498.
- (20) Karni, M.; Apeloig, Y.; Kapp, J.; Schleyer, P. v. R. Theoretical Aspects of Compounds Containing Si, Ge, Sn and Pb. *The Chemistry of Organic Silicon Compounds* **2001**, *3*, 1.
- (21) Tsuji, H.; Terada, M.; Toshimitsu, A.; Tamao, K. Sigma Sigma\* Transition in Anti,Cisoid Alternating Oligosilanes: Clear-Cut Evidence for Suppression of Conjugation Effect by a Cisoid Turn. *J. Am. Chem. Soc.* **2003**, *125*, 7486–7487.
- (22) Fukazawa, A.; Tsuji, H.; Tamao, K. All-Anti-Octasilane: Conformation Control of Silicon Chains Using the Bicyclic Trisilane as a Building Block. *J. Am. Chem. Soc.* **2006**, *128*, 6800–6801.
- (23) Kanazawa, Y.; Tsuji, H.; Ehara, M.; Fukuda, R.; Casher, D. L.; Tamao, K.; Nakatsuji, H.; Michl, J. Electronic Transitions in Conformationally Controlled Peralkylated Hexasilanes. *ChemPhysChem* **2016**, *17*, 3010–3022.
- (24) George, C. B.; Ratner, M. A.; Lambert, J. B. Strong Conductance Variation in Conformationally Constrained Oligosilane Tunnel Junctions†. *J. Phys. Chem. A* **2009**, *113*, 3876–3880.
- (25) Albinsson, B.; Teramae, H.; Downing, J. W.; Michl, J. Conformers of Saturated Chains: Matrix Isolation, Structure, Ir and Uv Spectra of N-Si4me10. *Chem. - Eur. J.* **1996**, *2*, 529–538.
- (26) Metzger, R. M. Unimolecular Electronics. *Chem. Rev.* **2015**, *115*, 5056–5115.
- (27) Su, T. A.; Neupane, M.; Steigerwald, M. L.; Venkataraman, L.; Nuckolls, C. Chemical Principles of Single-Molecule Electronics. *Nat. Rev. Mater.* **2016**, *1*, 16002.
- (28) Salomon, A.; Cahen, D.; Lindsay, S.; Tomfohr, J.; Engelkes, V. B.; Frisbie, C. D. Comparison of Electronic Transport Measurements on Organic Molecules. *Adv. Mater.* **2003**, *15*, 1881–1890.
- (29) McDermott, S.; George, C. B.; Fagas, G.; Greer, J. C.; Ratner, M. A. Tunnel Currents across Silane Diamines/Dithiols and Alkane Diamines/Dithiols: A Comparative Computational Study. *J. Phys. Chem. C* **2009**, *113*, 744–750.
- (30) Xu, B.; Tao, N. J. Measurement of Single-Molecule Resistance by Repeated Formation of Molecular Junctions. *Science* **2003**, *301*, 1221–1223.
- (31) Due to space constraints, we have not included a discussion of the preparation of the materials used in the studies described, but they can be found in the original publications. Likewise the STM measurement methods have been described in detail elsewhere.
- (32) Kumada, M.; Tamao, K. Aliphatic Organopolysilanes. *Adv. Organomet. Chem.* **1968**, *6*, 19–117.
- (33) Kumada, M.; Sakamoto, S.; Ishikawa, M. Organopolygermanes I.  $\alpha,\omega$ -Diphenylpolymethylpolygermanes. Preparation and Phenyl-dimethylgermyllithium-Catalyzed Disproportionation. *J. Organomet. Chem.* **1969**, *17*, 235–240.
- (34) Marschner, C. Preparation and Reactions of Polysilanyl Anions and Dianions. *Organometallics* **2006**, *25*, 2110–2125.
- (35) Luo, L.; Choi, S. H.; Frisbie, C. D. Probing Hopping Conduction in Conjugated Molecular Wires Connected to Metal Electrodes. *Chem. Mater.* **2011**, *23*, 631–645.
- (36) Klausen, R. S.; Widawsky, J. R.; Su, T. A.; Li, H.; Chen, Q.; Steigerwald, M. L.; Venkataraman, L.; Nuckolls, C. Evaluating Atomic Components in Fluorene Wires. *Chemical Science* **2014**, *5*, 1561–1564.
- (37) Klausen, R. S.; Widawsky, J. R.; Steigerwald, M. L.; Venkataraman, L.; Nuckolls, C. Conductive Molecular Silicon. *J. Am. Chem. Soc.* **2012**, *134*, 4541–4544.
- (38) Venkataraman, L.; Klare, J. E.; Nuckolls, C.; Hybertsen, M. S.; Steigerwald, M. L. Dependence of Single-Molecule Junction Conductance on Molecular Conformation. *Nature* **2006**, *442*, 904–907.
- (39) He, J.; Chen, F.; Li, J.; Sankey, O. F.; Terazono, Y.; Herrero, C.; Gust, D.; Moore, T. A.; Moore, A. L.; Lindsay, S. M. Electronic Decay Constant of Carotenoid Polyenes from Single-Molecule Measurements. *J. Am. Chem. Soc.* **2005**, *127*, 1384–1385.
- (40) Meisner, J. S.; Kamenetska, M.; Krikorian, M.; Steigerwald, M. L.; Venkataraman, L.; Nuckolls, C. A Single-Molecule Potentiometer. *Nano Lett.* **2011**, *11*, 1575–1579.
- (41) Su, T. A.; Li, H.; Klausen, R. S.; Widawsky, J. R.; Batra, A.; Steigerwald, M. L.; Venkataraman, L.; Nuckolls, C. Tuning Conductance in  $\pi$ - $\sigma$ - $\pi$  Single-Molecule Wires. *J. Am. Chem. Soc.* **2016**, *138*, 7791–7795.
- (42) Sommer, L. H.; Whitmore, F. C. Organo-Silicon Compounds. Iii. 1 A-and B-Chloroalkyl Silanes and the Unusual Reactivity of the Latter2. *J. Am. Chem. Soc.* **1946**, *68*, 485–487.
- (43) Whitmore, F. C.; Sommer, L. H. Organo-Silicon Compounds. Ii. 1 Silicon Analogs of Neopentyl Chloride and Neopentyl Iodide. The Alpha Silicon Effect1. *J. Am. Chem. Soc.* **1946**, *68*, 481–484.
- (44) Lambert, J. B. Tetrahedron Report Number 273: The Interaction of Silicon with Positively Charged Carbon. *Tetrahedron* **1990**, *46*, 2677–2689.
- (45) Su, T. A.; Li, H. X.; Klausen, R. S.; Widawsky, J. R.; Batra, A.; Steigerwald, M. L.; Venkataraman, L.; Nuckolls, C. Tuning Conductance in Pi-Sigma-Pi Single-Molecule Wires. *J. Am. Chem. Soc.* **2016**, *138*, 7791–7795.
- (46) Madelung, O. *Semiconductors: Data Handbook*; Springer Science & Business Media, 2012.
- (47) Su, T. A.; Li, H.; Zhang, V.; Neupane, M.; Batra, A.; Klausen, R. S.; Kumar, B.; Steigerwald, M. L.; Venkataraman, L.; Nuckolls, C. Single-Molecule Conductance in Atomically Precise Germanium Wires. *J. Am. Chem. Soc.* **2015**, *137*, 12400–12405.
- (48) Gu, G.; Burghard, M.; Kim, G.-T.; Düsberg, G.; Chiu, P.; Krstic, V.; Roth, S.; Han, W. Growth and Electrical Transport of Germanium Nanowires. *J. Appl. Phys.* **2001**, *90*, 5747–5751.
- (49) Barth, S.; Kolečník, M. M.; Donegan, K.; Krstic, V.; Holmes, J. D. Diameter-Controlled Solid-Phase Seeding of Germanium Nanowires: Structural Characterization and Electrical Transport Properties. *Chem. Mater.* **2011**, *23*, 3335–3340.
- (50) Mahenderkar, N. K.; Liu, Y.-C.; Koza, J. A.; Switzer, J. A. Electrodeposited Germanium Nanowires. *ACS Nano* **2014**, *8*, 9524–9530.
- (51) Hanrath, T.; Korgel, B. A. Influence of Surface States on Electron Transport through Intrinsic Ge Nanowires. *J. Phys. Chem. B* **2005**, *109*, 5518–5524.
- (52) Li, H.; Su, T. A.; Zhang, V.; Steigerwald, M. L.; Nuckolls, C.; Venkataraman, L. Electric Field Breakdown in Single Molecule Junctions. *J. Am. Chem. Soc.* **2015**, *137*, 5028–5033.
- (53) Li, H.; Kim, N. T.; Su, T. A.; Steigerwald, M. L.; Nuckolls, C.; Darancet, P.; Leighton, J. L.; Venkataraman, L. Mechanism for Si–Si Bond Rupture in Single Molecule Junctions. *J. Am. Chem. Soc.* **2016**, *138*, 16159–16164.
- (54) Paul, D. J. Si/Sige Heterostructures: From Material and Physics to Devices and Circuits. *Semicond. Sci. Technol.* **2004**, *19*, R75.
- (55) Myers, A. G.; Kephart, S. E.; Chen, H. Silicon-Directed Aldol Reactions. Rate Acceleration by Small Rings. *J. Am. Chem. Soc.* **1992**, *114*, 7922–7923.
- (56) Denmark, S. E.; Griedel, B. D.; Coe, D. M. The Chemistry of Enoxy-silacyclobutanes: Highly Selective, Uncatalyzed Aldol Additions. *J. Org. Chem.* **1993**, *58*, 988–990.
- (57) Matsumoto, K.; Oshima, K.; Utimoto, K. Noncatalyzed Stereoselective Allylation of Carbonyl Compounds with Allylsilacyclobutanes. *J. Org. Chem.* **1994**, *59*, 7152–7155.
- (58) Su, T. A.; Widawsky, J. R.; Li, H.; Klausen, R. S.; Leighton, J. L.; Steigerwald, M. L.; Venkataraman, L.; Nuckolls, C. Silicon Ring Strain Creates High-Conductance Pathways in Single-Molecule Circuits. *J. Am. Chem. Soc.* **2013**, *135*, 18331–18334.
- (59) Kim, N. T.; Li, H. X.; Venkataraman, L.; Leighton, J. L. High-Conductance Pathways in Ring-Strained Disilanes by Way of Direct Sigma-Si to Au Coordination. *J. Am. Chem. Soc.* **2016**, *138*, 11505–11508.
- (60) Joost, M.; Gualco, P.; Coppel, Y.; Miqueu, K.; Kefalidis, C. E.; Maron, L.; Amgoune, A.; Bourissou, D. Direct Evidence for Intermolecular Oxidative Addition of  $\Sigma$  (Si–Si) Bonds to Gold. *Angew. Chem., Int. Ed.* **2014**, *53*, 747–751.
- (61) Su, T. A.; Li, H.; Steigerwald, M. L.; Venkataraman, L.; Nuckolls, C. Stereoelectronic Switching in Single-Molecule Junctions. *Nat. Chem.* **2015**, *7*, 215–220.
- (62) Our nomenclature refers to the disposition of the Me group rather than the Au atom.